J. Am. Chem. Soc. **1987**, *109*, 3251–3257

Electrocatalysis of Oxygen Reduction by Chalcogenides Containing Mixed Transition Metal Clusters

N. Alonso Vante,† W. Jaegermann,† H. Tributsch,*† W. Hönle,‡,§ and K. Yvon‡

Contribution from the Hahn-Meitner-Institut, D-1000 Berlin 39, West Germany, and the Laboratoire de Cristallographie aux Rayons X, Université de Genève, CH 1211 Geneva, Switzerland.

Received September 22, 1986

Abstract: A new class of catalysts for the reduction of molecular oxygen to water in acid environment has been discovered, which show electrocatalytical activity comparable to that of platinum. They are Chevrel type chalcogenides with the stoichiometry $Mo_{6-x}M_xX_8$ (M = transition metal, X = chalcogen atom), containing octahedral mixed-metal clusters of transition-metal atoms. Experimental data obtained with rotating disk and rotating ring disk techniques, photoelectrochemical studies, photoelectron spectroscopy, and conductivity measurements are presented for the compound $Mo_{4.2}Ru_{1.8}Se_8$, which is a p-type semiconductor (energy gap determined to be $E_g = 1.3$ eV). The catalytic activity increases from samples containing nonsubstituted Mo octahedra showing metallic behavior to samples containing Ru substituted Mo octahedra showing semiconducting behavior due to an electron count close to 24. Possible mechanisms of catalysis are discussed. Important features are considered to be the capacity of the cluster to act as a reservoir for electronic charge carriers while maintaining a stable electrochemical potential, its capacity to provide neighboring binding sites for reactants and intermediates, and its ability to change its volume and bonding distances in the course of electron transfer.

I. Introduction

Electrocatalytic properties of Chevrel phases $Mo_{6-x}M_xX_8$ (M = transition metal, X = chalcogen) containing mixed-metal clusters ($Mo_{6-x}M_x$)[1] have recently been reported in a short communication.[2] This work is part of a research effort to identify new catalytic materials for generation of chemical fuels in photoelectrochemical solar cells. For this purpose semiconducting transition-metal compounds which provide sufficient high densities of metal states at the band edges have proven to be most promising.[3-5] In this class of materials charge carriers (holes and electrons, respectively), which are necessary to bind reactants and intermediates during multielectron transfer reactions, are expected to induce coordination chemistry at the electrode surface. All semiconducting d-band materials so far tested (dichalcogenides of Mo, W, Re, Fe, Pt, Ru) that fulfill this condition actually photoreact with water. However, only disulfides of transition metals which are able to reach high oxidation states (Pt, Ru) are able to photoevolve molecular oxygen from water.[6,7] Since no cooperative reaction between neighboring transition metal atoms is possible in these dichalcogenides due to their large interatomic distances, individual transition-metal atoms have to successively capture four holes while oxidizing two OH^- ions via a peroxo-type complex to molecular oxygen. In contrast, transition-metal atoms which cannot reach sufficiently high oxidation states, e.g., Fe, react with OH^- but pass the bound oxygen on to the chalcogenide ligands.

The presently most efficient electrode for potential assisted photoevolution of oxygen from water, RuS_2 ($E_g = 1.2$ eV), evolves molecular oxygen with a quantum efficiency between 10 and 60% while remaining stable against photocorrosion.[7] The decrease of the ability for oxygen evolution in the series RuS_2, $RuSe_2$, $RuTe_2$, combined with a simultaneous increase of corrosion, goes parallel with an increase of mixing between Ru states at the edge of the valence band and the lower chalcogen states.[8] This emphasizes the role of d-states in the multielectron reaction leading to the evolution of molecular oxygen. RuS_2, although it forms a thin oxide film (approximately two monolayers) during oxygen evolution, does not photoevolve oxygen at an overpotential as low as that for oxygen evolution at RuO_2 approximately 0.2 V). An overpotential of 0.6–0.7 occurs at RuS_2 because the capture of four holes by individual transition-metal atoms during the coordination of two OH^- ions is accompanied by a corresponding negative shift of electronic levels from which holes react with (OH^-/O_2).[9] Speaking in interfacial chemical terms, photogenerated holes are reacting with water by way of surface states (surface transition-metal complexes) which are shifted high up into the region of the forbidden energy gap. A reasonable way to overcome such an electronic relaxation appeared to be the utilization of semiconducting chalcogenides which contain clusters of transition-metal atoms.[9,10] Due to the increased delocalization of electrons in such clusters the relaxation of electronic states would be attenuated. In addition cooperative reactions of reactants bonded to neighboring transition-metal sites of the cluster would be possible. This investigation deals with an electrocatalytical study of a semiconducting mixed cluster compound which appears to fulfill these requirements. The study of additional, catalytically less favorable non-mixed cluster compounds was included for comparison.

II. Experimental Section

1. Sample Preparation. The following four samples were prepared: two containing pseudobinary selenides of composition $Mo_{4.2}Ru_{1.8}Se_8$ and $Mo_{3.7}Ru_{2.3}Se_8$ containing Ru-substituted ($Mo_{6-x}Ru_x$) clusters, and two ternary, Ni based tellurides of composition $Ni_{0.85}Mo_6Te_8$ (batch a and batch b) containing nonsubstituted Mo_6 clusters.

The Ru-containing samples were supplied by Dr. R. Baillif. They were prepared by the sintering of mixtures of high-purity elements in sealed quartz tubes at 1470 K, followed by melting at 1970 K in a high-pressure (0.7 GPa) argon furnace.[11] The weight loss during melting was small (only about 3 wt. %[12]). As shown by X-ray Guinier photographs and metallographic inspection the samples contained almost exclusively the rhombohedral phase described previously,[1,13] the estimated amount of impurity phases (nonidentified) being only about 4%.

---

† Hahn-Meitner-Institut.

‡ Université de Genève.

§ Permanent address: Max-Planck-Institut für Festkörperforschung, Heisenbergstrasse 1, D 7000 Stuttgart, Germany.

(1) Perrin, A.; Chevrel, R.; Sergent, M.; Fischer, O. *J. Solid State Chem.* **1980**, *33*, 43.

(2) Alonso Vante, N.; Tributsch, H. *Nature (London)* **1986**, *323*, 431.

(3) Tributsch, H. *Z. Naturforsch.* **1977**, *32a*, 972.

(4) Tributsch, H. *J. Electrochem. Soc.* **1978**, *125*, 169.

(5) Tributsch, H. *Structure and Bonding* **1982**, *49*, 128.

(6) Tributsch, H.; Gorochov, O. *Electrochim. Acta* **1982**, *27*, 2, 215.

(7) (a) Kühne, H.-M.; Tributsch, H. *J. Electrochem. Soc.* **1983**, *130*, 1448. (b) Kühne, H.-M.; Tributsch, H. *Ber. Bunsenges. Phys. Chem.* **1984**, *88*, 10. (c) Kühne, H.-M.; Tributsch, H. *J. Electroanal. Chem.* **1986**, *201*, 263.

(8) Kühne, H.-M.; Jaegermann, W.; Tributsch, H. *Chem. Phys. Lett.* **1984**, *112*, 160.

(9) Tributsch, H. *J. Photochem.* **1985**, *29*, 89.

(10) Tributsch, H. In *Modern Aspects of Electrochemistry*; Bockris, J. O'M., Conway, B. E., White, R. E., Eds.; Plenum Press: New York, London, 1986; Vol. 17, 303.

(11) Baillif, R. Ph.D. Thesis No. 2025, Université de Genève, 1982.

(12) Baillif, R., personal communication, 1982.

(13) Hönle, W.; Flack, H. D.; Yvon, K. *J. Solid State Chem.* **1983**, *49*, 157.

0002-7863/87/1509-3251$01.50/0

The Ni-containing samples were prepared by reaction of binary Mo_6Te_8 and elemental Ni powder at 1300 K in sealed, evacuated quartz tubes. The reaction products were sintered blocks containing 0.5 mol % elemental Ni as shown by magnetic susceptibility measurements. They appeared to be insensitive to moisture and air. Further details are given in ref 14.

2. Photoelectrochemical Apparatus and Electrode Preparation. For the recording of current–voltage curves, a standard (photo)electrochemical arrangement with a one-compartment three-electrode cell was employed. Potentiostate: (PAR) Model 273 or RDE3 (Pine Instrument). Two-phase lock-in amplifier (PAR): Model 5206. XYY′ recorder (Philips): PM-8134. Chopper (PAR): Model 9479. The spectral dependence of photocurrents was measured with a computer-controlled HP85 and the (PAR) apparatus, in connection with a VIS, IR grating monochromator (Kratos). The VIS, IR light source was provided from a W-Hal 250 W Lamp. Potentials were measured against a saturated calomel electrode (SCE) which was connected to the cell compartment through a liquid junction bridge with a high porosity ceramic tip. In the following, all potentials are referred to NHE. Analytical grade pure reagents and triply distilled water were used. The experiments were carried out at room temperature.

The cluster materials were cut from sintered blocks ($Ni_{0.85}Mo_6Te_8$), or ingots ($Mo_{6-x}Ru_xSe_8$) approximately 1 mm thick, and shaped into disks on a minigrill with an abrasive paper. They were back-ohmic contacted with a silver epoxy paste (Scotchcast 3M) and mounted on brass shafts for the rotating disk electrode (RDE) configuration. Insulating epoxy (Scotchcast 3M) was used to encapsulate the crystals on Vespel holders for the RDE (Tacussel Mod. EDI). The exposed electrode surfaces were not further polished mechanically, thus a very rough surface developed during this procedure. The electrodes were used as cut, washed with acetone and distilled water. Their electrochemical stability was tested by scanning (0.5–1 h) in the region of charging current in well outgassed solution with nitrogen, prior to the saturation of solution with high-purity oxygen. For the rotating ring disk electrode (RRDE) configuration, the disk, already mounted on a steel screw, was adjusted to give the best planarity relative to the concentric platinum ring; the gap between the ring and the disk was filled with epoxy. A (Jaissle) PI regler Model SR374 was used to drive this electrode. The experimental collection efficiency, N, of this electrode was 0.31 (theoretical value, N = 0.32). The hydrodynamics of this electrode was consistent up to 900 rpm in a 10^{-3} M $[Fe(CN)_6]^{-3}$ solution.

3. Resistivity Measurements. The DC resistance was measured in the temperature range 80–300 K. The samples ($Mo_{4.2}Ru_{1.8}Se_8$, $Mo_{3.7}Ru_{2.3}Se_8$) were mounted on a copper plate in an evacuated chamber for heating or cooling. Temperature control was provided by a calibrated resistor. The resistance was determined from the voltage bias under current flow.

4. XPS Measurements. Photoelectron spectra measurements were performed in a commercial UHV-multitechnique system (VG ESCALAB Mk II). As excitation sources, a He resonance lamp operating in the He I (21.2 eV) and He II (40.8 eV) mode and a non-monochromatized dual X-ray anode (Mg Kα line, 1253.6 eV) were used. The UP spectra were related to the Fermi edge of clean polycrystalline Au. The XP spectra were calibrated to the Au $4f_{7/2}$ (E_B (binding energy) = 83.8 eV) and Ag $3d_{5/2}$ (E_B = 368.0 eV) levels, respectively. The samples were attached by silver epoxy to copper screws to assure spatial isolation.

III. Results

1. Solid State and Photoelectrochemical Studies. The crystal structure of $Mo_{6-x}Ru_xSe_8$ containing mixed (Mo, Ru) clusters, is shown in Figure 1. The idealized coordination of the $(Mo,Ru)_6Se_8$ unit is more clearly presented in the upper part of the figure. It is characterized by an octahedron of metal atoms with the eight chalcogenides triply coordinated above the trigonal planes. The mean metal–metal distance is 2.684 Å, which indicates strong metal–metal interaction. The structure of $Ni_xMo_6Te_8$ is similar except that the Ni atoms occupy the chalcogen atom channels.

Semiconducting properties in the non-stoichiometric compounds $Mo_{4.2}Ru_{1.8}Se_8$ (23.6 cluster electrons) and $Mo_{3.7}Ru_{2.3}Se_8$ (24.6 cluster electrons) are confirmed by resistivity measurements as a function of temperature (Figure 2). Both compounds show decreasing resistivity with increasing temperature as is typical for semiconducting samples. However, as is suggested by the flat slope of the curves and the high conductivity of the samples, the non-stoichiometric compounds are degenerate semiconductors. This result can be rationalized by comparing the actual number of electrons available (based on the determined stoichiometry) with the number to fill up all available bonding cluster electron states (24 cluster electrons). In one case the conduction band contains a surplus of electrons (0.6 per mol), and in the other case the lack of bonding electrons leads to a surplus of holes in the valence band (0.4 per mol). For the latter compound ($Mo_{4.2}Ru_{1.8}Se_8$) small cathodic photocurrents, which are typical for p-type semiconductors, were observed in contact with an acid aqueous electrolyte (approximately 1 μA cm^{-2} at 10 mW cm^{-2} of tungsten light). They nevertheless permitted the measurement of a photoaction spectrum (Figure 3). It shows an energy gap of E_g = 1.3 eV (0.2 eV bigger than for $MoSe_2$) and a structured absorption edge. To our knowledge this is the first time that an energy gap determination has been published for a semiconducting Chevrel phase mixed metal cluster compound. The results appear to be in quite good agreement with theoretical calculations by Mattheiss and Fong,[15]

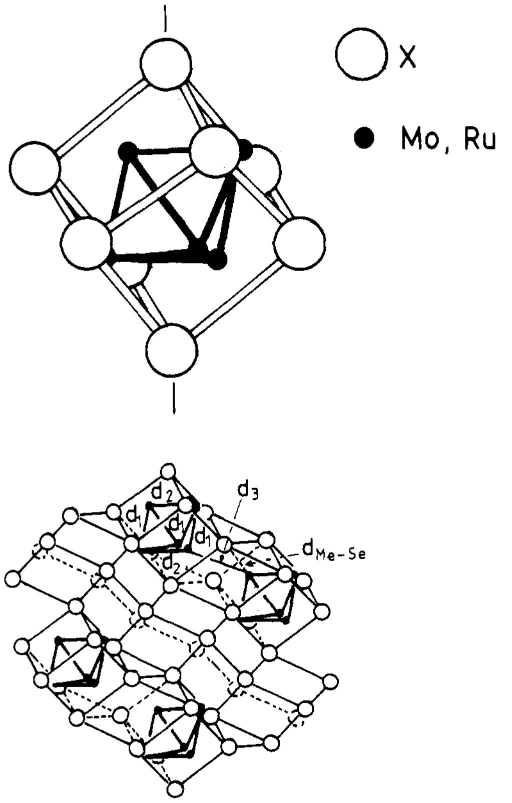

Figure 1. Structure of $(MoRu)_6Se_8$. Metal atom octahedra are represented with heavy lines and Se atoms by circles (adapted from ref 13).

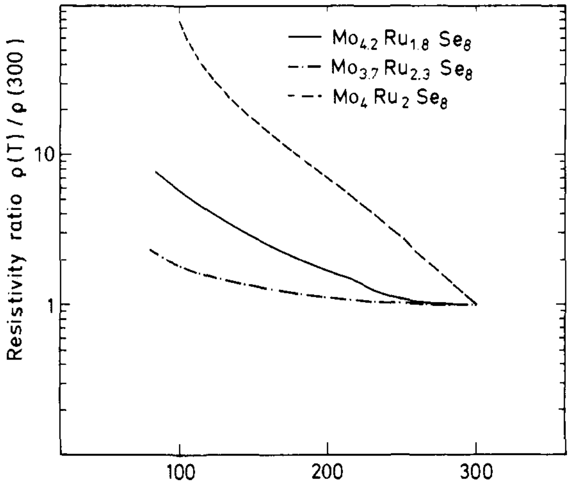

Figure 2. Normalized resistivity of $Ru_{6-x}Mo_xSe_8$ compounds as a function of the absolute temperature. $Mo_4Ru_2Se_8$ adapted from ref 1.

---

(14) Hönle, W.; Yvon, K. *J. Solid State Chem.*, submitted for publication.

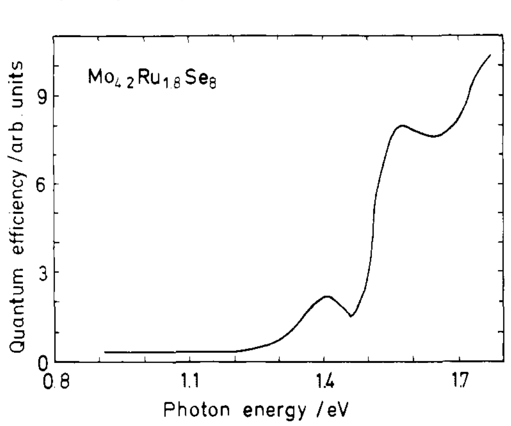

Figure 3. Relative quantum efficiency vs. photon energy for $Mo_{4.2}Ru_{1.8}Se_8$ in 0.5 M H_2SO_4 solution. Chopping frequency 70 Hz.

which predicted for the Mo_6S_8 cluster a gap amounting to 0.11–0.13 Ry (1.49–1.76 eV) separating 30 Mo 4d MO levels into a lower nearly filled subgroup of 12 states (metallic conduction) and an upper unoccupied manyfold of 18 levels. The gap thus separates the nearly filled weakly bonding Mo 4d MOs from the upper unoccupied antibonding states. Recently Nohl, Klose, and Andersen provided an improved calculation[16] for this type of cluster compounds. Replacement of two Mo atoms for Ru should fill up the lower weakly bonding states forming the valence band of the semiconducting $Mo_4Ru_2Se_8$ compound. However, we cannot exclude the idea that the presence of Ru and Se as in our $Mo_{4.2}Ru_{1.8}Se_8$ compound will distort the described electronic structure and the size of the predicted energy gap.

2. Photoelectron Spectroscopy. In order to obtain additional information on the electronic properties of the material and especially on the electronic structure of the valence band which is involved in the electron exchange at the interface of a p-type electrode in the dark, surface analytical studies of both pure and treated samples were performed by electron spectroscopy (XPS,UPS). For this purpose it is a precondition to obtain clean and uncontaminated surfaces. As for most other transition-metal chalcogenides Ar^+ etching leads to a preferential sputtering of Se thus changing the stoichiometry very drastically. Therefore an attempt was made to clean the surface of the samples by scratching them mechanically with a blade inside the UHV system. This technique proved to be successful. The surfaces obtained were free of contamination with respect to XPS analysis and show sharp bands of Mo, Ru, and Se of the same intensity ratio as observed before the scratching treatment. Both compounds show very similar spectra, therefore in the following only the spectra of the Ru-rich species are presented.

Valence band spectra obtained for He I (21.2 eV), He II (40.8 eV), and Mg Kα (1253.6 eV) excitation are shown in Figure 4. The prominent bands in the UV–photoelectron spectra are found at 1.9, 3.0, 5.2, and 6.2 eV (with respect to $E_F = 0$). In the X-ray photoelectron spectra the first two peaks are convoluted into one band at 2.2 eV and the other peaks are present as shoulders on a broad band centered around 4.6 eV. On the basis of the already cited MO calculations of isolated Mo_6X_8 cluster units as well as of band structure calculations of Chevrel phases[15,16] these bands are assigned to transition-metal d states (1.9, 3.0 eV) and Se 4p states (5.2, 6.5 eV). The Se 4s states show up as a band at ~14 eV in the XP spectrum. This assignment is supported by the peak intensity dependence on the excitation wavelength. The photoionization cross section of d electrons tends to increase with increasing excitation energy in contrast to p electrons.[17] Correspondingly the intensity of the first two peaks increase considerably when changing from He I to He II excitation. The d bands result from metal–metal interactions in the $(Mo,Ru)_6$ octahedron and can be considered as filled weakly bonding MO's (the bonding states, which are essentially responsible for the structural stability, are the Se 4s and 4p states). The antibonding d states form the conduction band of the semiconducting cluster compound. The resulting electronic structure is qualitatively given in Figure 4b. When the different electron count when changing from pure Mo octahedra (20 e^-) to Ru-substituted octahedra (24 e^- for substitution of 2 Mo atoms) is disregarded, the binding energies of d electrons for the transition metals in both compounds are presumably similar.[18] A factor which could lead to differences is a change in the cluster geometry due to atomic size and band filling effects as shown[13] recently for the mixed metal cluster compound $Mo_4Ru_2Se_8$ and $Mo_{1.5}Re_{4.5}Se_8$.

The different proportions of transition metals in the two presently investigated mixed metal cluster compounds $Mo_{4.2}Ru_{1.8}Se_8$ and $Mo_{3.7}Ru_{2.3}Se_8$ are more clearly reflected in the XP spectra of the core electrons (Figure 5a). The relative intensities of the Mo $3d_{5/2}$:Ru $3d_{5/2}$:Se 3d levels are 5.5:1.3:8 and 4.5:1.8:8. These intensity ratios, calculated after correction by theoretical photoionization cross sections,[19] show in both cases a smaller surface concentration of Se. The binding energy values reported for the main lines (fwhm ~ 1.4 eV) of Se (E_B(3d): 54.2 eV), Mo ($E_B(3d_{5/2})$: 228.3 eV), and Ru ($E_B(3d_{5/2})$: 280.1 eV) are in reasonable agreement with the values reported for layer-type and cubic transition metal dichalcogenides.[20,21]

Samples stored in air are oxidized as can be derived from broadening of bands (Figure 5b) and additional peaks which can be related to the formation of MoO_3 (E_B Mo $(3d_{5/2})$: 232.6 eV).[22] It is not clear whether Ru is also oxidized, since a similar E_B value is measured as in the non-oxidized samples, but we cannot exclude the fact that the ruthenium dioxide peak is hidden in the Ru peak of the cluster. The O 1s level shows up as a broad band (fwhm ~ 4 eV) at E_B = 532 eV, which evidently is composed of oxide/hydroxide (E_B ~530–531 eV[20]) and water (E_B ~533 eV[20]) contributions. There is no evidence for the formation of Se oxide compounds on the surface. The oxidation products (at 1.24 V, polarization 2 min) formed in acidic as well as neutral aqueous solution and subsequent rinsing with distilled water gave very similar results (Figure 5c). There is an increased contribution of MoO_3 and additional contribution due to SeO_2 (E_B (Se 3d): - 59 eV) and RuO_3/RuO_4^- (E_B(Ru $3d_{5/2}$): ~282 eV).[19,22] For the O 1s level a E_B value of 531 eV was measured, which also indicates the presence of oxides at the surface. These anodically formed oxides can be reduced again at potentials smaller than 0.84 V. Electrodes that are analyzed after polarization at 0.24 V for 4 min show no more contributions of oxides at the surface. However, the relative intensity of the Mo and Se lines is decreased in comparison with Ru. Evidently, MoO_3 and SeO_2, which both are soluble as anions, are preferentially dissolved. This is in agreement with electrochemical results which show, for a constant potential sweep ($0.06 < U < 1.24$ V), gradually rising anodic and cathodic currents (see below). This is not the case for samples, which after surface cleaning are directly polarized in the potential region of oxygen reduction ($0.04 < U < 0.84$ V). For these electrodes, even after extensive reduction time ($t > 2$ h) no evidence is found for any changes in the spectra either with respect to any additional species formed or with respect to the element ratios. It is therefore justified to conclude that the $(Mo,Ru)_6Se_8$ compounds are stable during oxygen reduction.

3. Electrochemical Studies of Oxygen Reduction. Cyclic voltammograms of $Mo_{4.2}Ru_{1.8}Se_8$ are shown in Figure 6. First, the potential range was increased at a constant scanning rate up to 1.24 V. From then on the 1st, the 4th, and the 10th cycles were recorded. The graphs show that following an anodic increase of the current there is an increase of the cathodic current which

---

(15) Mattheiss, L. F.; Fong, C. Y. *Phys. Rev. B* **1977**, *15*, 1760.

(16) Nohl, H.; Klose, W.; Andersen, O. K. In *Superconductivity in Ternary Compounds I*; Fischer, Ø., Maple, M. B., Eds.; Springer Verlag: West Berlin, 1982; p 165.

(17) Manson, S. T. In *Topics in Applied Physics*; Ley, L., Cardona, M., Eds.; Springer Verlag: West Berlin, 1979; pp 26 and 27.

(18) Lotz, W. *J. Opt. Soc. Am.* **1970**, *60*, 206.

(19) Scofield, J. H. *J. Electron. Spectrosc.* **1976**, *8*, 129.

(20) Jaegermann, W.; Schmeisser, D. *Surf. Sci.* **1986**, *165*, 143.

(21) Jaegermann, W.; Kühne, H.-M. *Appl. Surf. Sci.* **1986**, *26*, 1.

(22) *Handbook of X-Ray Photoelectron Spectroscopy*; Muellenberg, G. E., Ed.; Perkin-Elmer, Physical Electronics Division: Eden Prairie, NY, 1979.

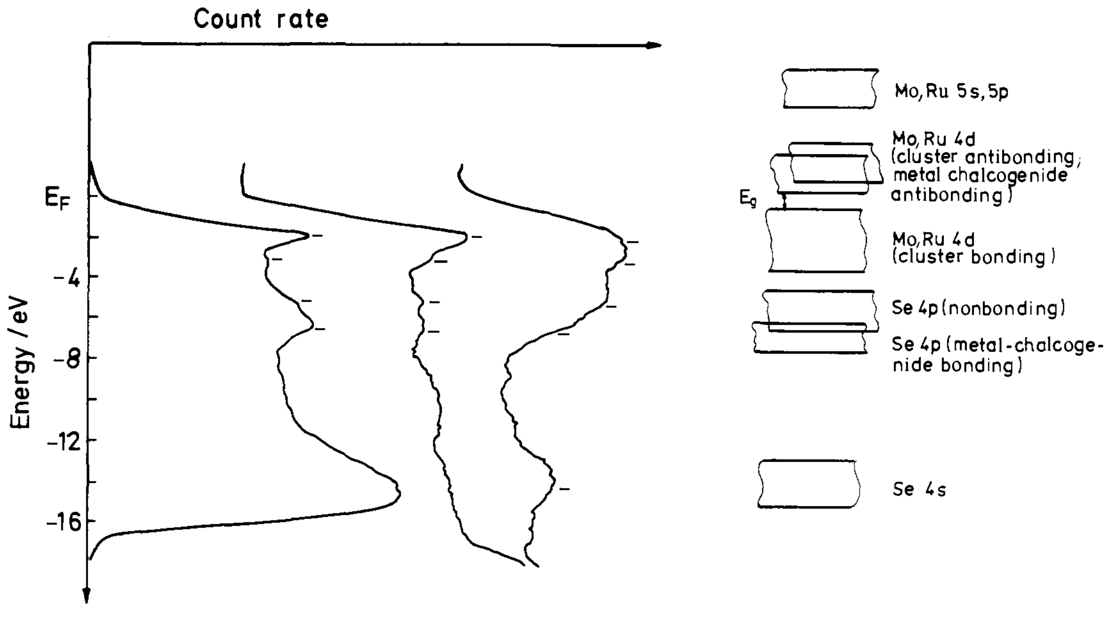

(a) (b)

Figure 4. (a) Valence band spectra of $Mo_{3.7}Ru_{2.3}Se_8$: the energy scale is referred to the Fermi energy ($E_F = 0$), see text for spectral features. (b) Qualitative energy band diagram of the corresponding spectra.

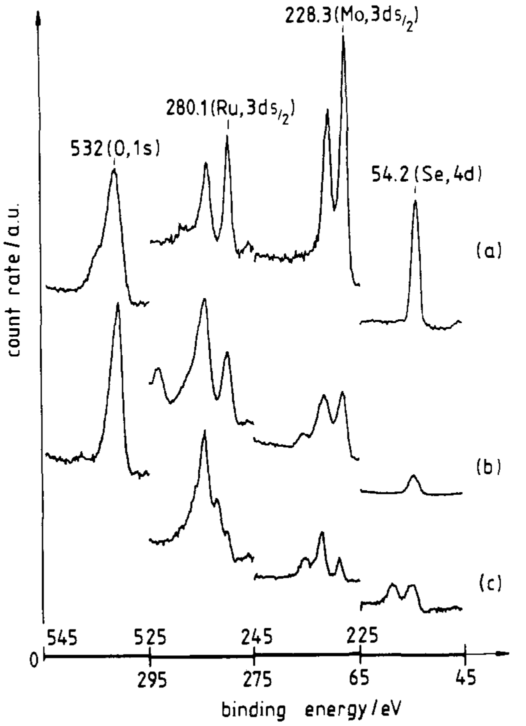

Figure 5. ESCA spectra for the $Mo_{3.7}Ru_{2.3}Se_8$ sample in the regions of d lines of Se, Mo, Ru and the s line of O, respectively: (a) scratched surface, (b) surface exposed in air, (c) surface treated electrochemically in 0.5 M H_2SO_4 at +1.24 V.

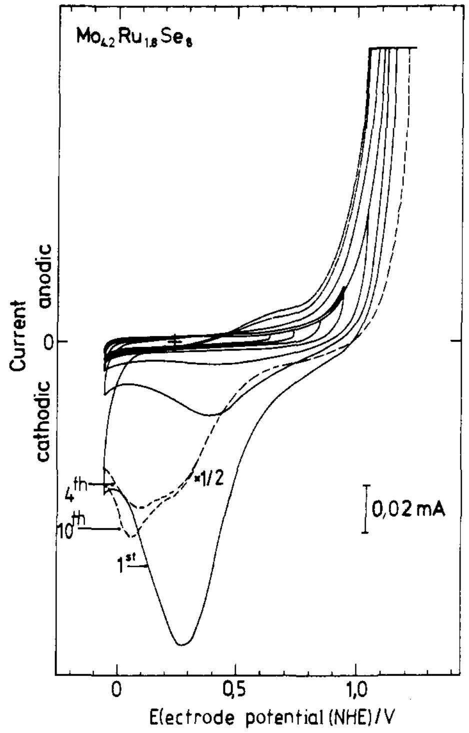

Figure 6. Cyclic voltammetry current vs. potential profiles for $Mo_{4.2}Ru_{1.8}Se_8$ compound at 0.1 V s^{-1} in 0.5 M H_2SO_4 under nitrogen atmosphere. 1st, 4th, and 10th represent the number of scans for one profile, i.e., −0.06 to +1.24 V.

indicates an anodic dissolution of oxidation products. The fact that dissolution occurs is confirmed by XPS data, see later, and the accumulation of the oxidation products in the electrolyte. This corrosion phenomenon is observable only at electrode potentials bigger than 0.84 V. With the sample $Mo_{3.7}Ru_{2.3}Se_8$ the same pattern was observed. However, less corrosion was apparent (smaller turnover of charge during reduction) and a satellite peak appeared, which indicates an altered interfacial chemistry.

The electrochemical reduction curves in both the absence and presence of oxygen, determined for the ternary Ni containing and the two pseudobinary $(Mo,Ru)_6$ mixed cluster compounds, are shown in Figure 7. All these materials catalyze the reduction of oxygen in acid medium, but the potential of the disk current measured vary markedly as a function of the composition. Interestingly, although at potentials more negative, the reduction of oxygen proceeds with both batches of the Ni based ternary compounds (Figure 7a,b). The difference in behavior between the two batches of nominal stoichiometry of $Ni_{0.85}Mo_6Te_8$ was due to the unequal Ni concentration on the electrode surface, as proved by scanning electron microscopy and X-ray fluorescence analysis. For the batch (b) a Ni concentration at the electrode surface of the order of 30% higher was found. Nickel compounds are known to be inactive in acid but moderately active in alkaline medium.[23]

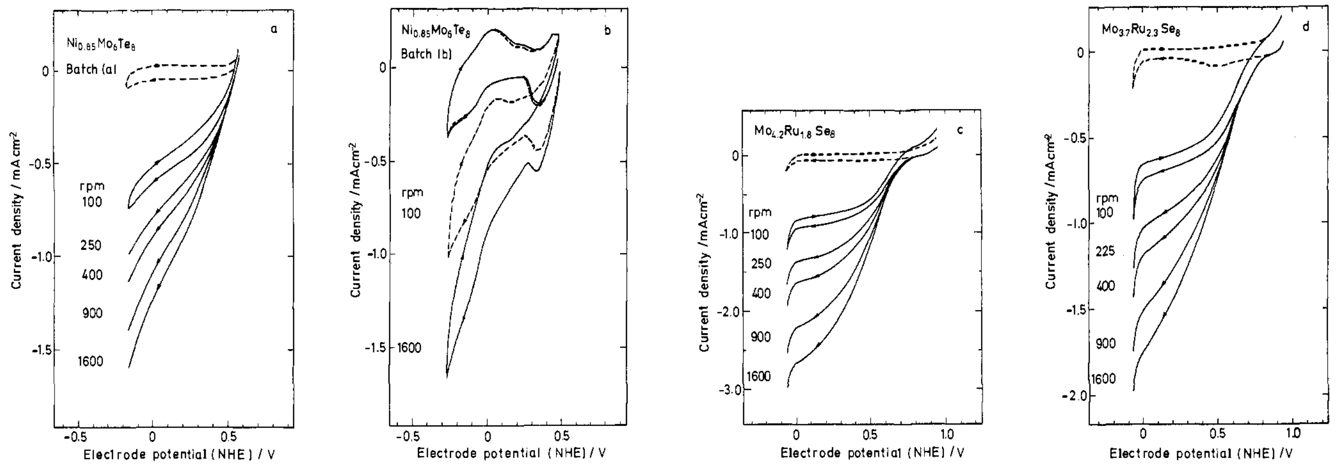

Figure 7. Current–potential curves for the reduction of O_2 at rotating disk electrodes: (a) $Ni_{0.85}Mo_6Te_8$ (batch a); (b) $Ni_{0.85}Mo_6Te_8$ (batch b); (c) $Mo_{4.2}Ru_{1.8}Se_8$; (d) $Mo_{3.7}Ru_{2.3}Se_8$. Rotation rates are indicated (rpm). Electrolyte (0.5 M H_2SO_4) was saturated with O_2. Electrode potentials were scanned at 5 mV s^{-1}. Background curves obtained in the same solution but saturated with nitrogen, not labeled (rpm), are also represented.

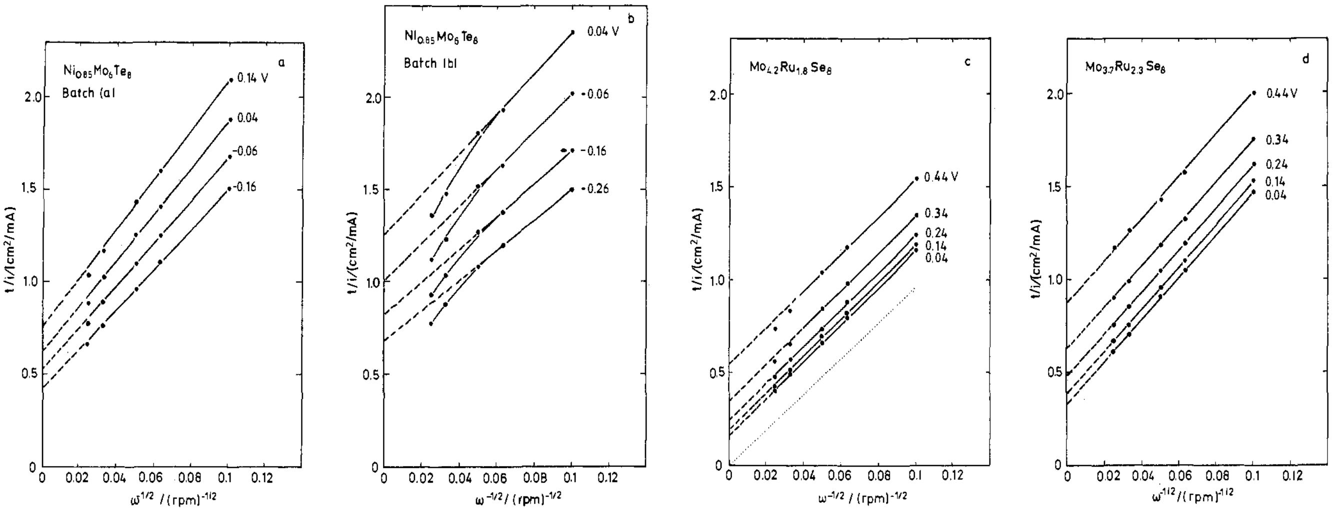

Figure 8. Koutecky–Levich plots from the RDE data represented in Figure 7. The theoretical slope for a 4-electron transfer is represented by the dotted line in (c).

On the other hand, the compounds containing ruthenium-substituted Mo_6 clusters showed a remarkable catalytic activity (Figure 7c,d). The magnitude of the reduction current for $Mo_{4.2}Ru_{1.8}Se_8$ is, under identical transport conditions, 30% bigger than that for the compound $Mo_{3.7}Ru_{2.3}Se_8$ which contains more Ru. For both, the overpotential is not higher than 0.35 V (measured with a current density of 10^{-5} A cm^{-2} with respect to the thermodynamic potential $E_0(O_2/H_2O) = 1.21$ V/NHE (pH = 0.3)). The analysis of these curves showed that the observed currents are related to the rotation rate by $1/i = 1/i_k + 1/B\omega^{1/2}$ (i_k = kinetic current, $B\omega^{1/2} = i_d$, the corresponding diffusion limited current).

The Koutecky–Levich plots were obtained in the following way: after measuring the base line (dotted curves in Figure 7a–c) in nitrogen-degassed solution, the current densities for O_2 reduction were then determined at different potentials during a quasidynamic sweep into the negative potential direction (5 mV/s). This type of plot yielded parallel straight lines for the catalysts $Mo_{4.2}Ru_{1.8}Se_8$ and $Mo_{3.7}Ru_{2.3}Se_8$ in the range of 0.44–0.04 V (Figure 8c,d). Such a behavior is not found for the Ni-based samples. Their slopes B vary 20% in the range of −0.16 to 0.14 V for batch (a) and 25% in the range of −0.26 to 0.04 V for batch (b). Measurements at more negative potential, with the Ru-based samples, which should have yielded straight lines crossing the origin, were not justified due to the onset of proton reduction (formation of bubbles). Qualitatively these results show for the ruthenium-containing cluster a first-order kinetics with respect to the diffusing reactant. On the Ni-containing cluster compound the nonlinearity of experimental points and the lack of parallelism could indicate the contribution of mixed reaction pathways.

In view of the intercept of the $1/i$ plot with $\omega^{-1/2} \rightarrow 0$ which is a measure of the catalytic activity of the electrode material, sample $Mo_{4.2}Ru_{1.8}Se_8$ appears to be the best catalyst and thus will now be further analyzed; the theoretical slope (calculated for $c_{O_2} = 1.1 \times 10^{-6}$ gmol cm^{-3}, $D_{O_2} = 1.4 \times 10^{-5}$ cm^2 s^{-1}, $\nu = 0.01$ cm^2 s^{-1})[24] for an electron-transfer reaction involving approximately four electrons can be seen to be very similar to the experimental one (Figure 8c, dotted line). In order to further confirm that O_2 is directly reduced to H_2O, RRDE experiments were performed with the aim of tracing H_2O_2 as an intermediate. Figure 9 shows the result obtained. An analysis of the very small ring current, I_R, and disk current, I_D, normalized for the collection efficiency, N, shows that only 2.8–3.9% of hydrogen peroxide is formed during oxygen reduction to water in acidic medium. This has to be considered as an exceptional behavior for a semiconductor and testifies for the excellent catalytic performance of this transition-metal cluster material. For a further experimental confirmation of our results we have performed RRDE studies with Pt

---

(23) Tarasevich, A. R.; Sadkowsky, A.; Yeager, E. In *Comprehensive Treatise of Electrochemistry*; Conway, B. E., Bockris, J. O'M., Yeager, E., Khan, S. U. M., White, R. Eds.; Plenum Press: New York, London, 1983; Vol. 7, p 301.

(24) Hsueh, K.-L.; Gonzalez, E. R.; Srinivasan, S. *Electrochim. Acta* **1983**, *12*, 691.

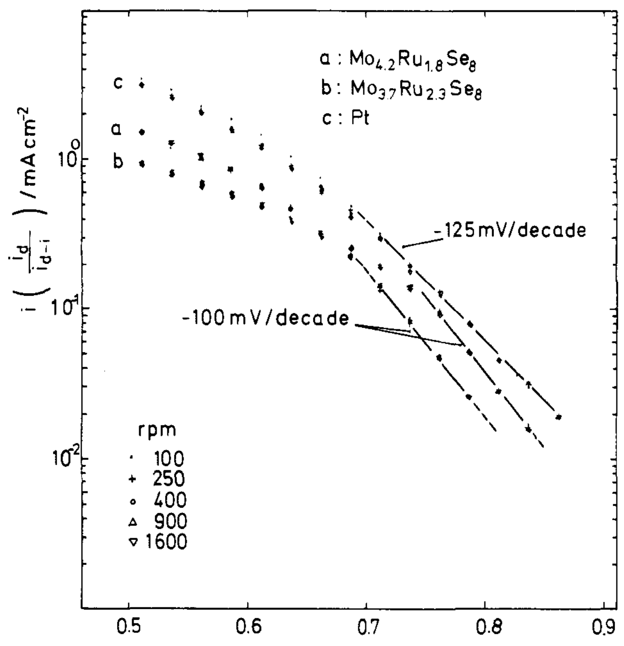

Figure 9. Corrected mass transfer Tafel plots for O_2 reduction at various rotation rates for $Mo_{4.2}Ru_{1.8}Se_8$ and $Mo_{3.7}Ru_{2.3}Se_8$ in 0.5 M H_2SO_4. For the sake of comparison, the curve obtained with the platinum electrode is also represented for the same condition.

at exactly the same experimental conditions. The lowest hydrogen peroxide yield (dependent on surface treatment and history) obtained was 4%, which is lower than most values reported in the literature (3–20%).[25] This comparison places the catalytic activity of the mixed metal $(Mo,Ru)_6$ cluster compound on the same level as that of platinum.

More kinetic information on the electron transfer reaction mediated by $(Mo,Ru)_6Se_8$ is displayed in Figure 9. It shows Tafel plots (U/log i) after mass transfer correction and within an accuracy of 6%. This Tafel behavior is independent of the rotation frequency and covers the range from 100 to 1600 rpm. The slopes obtained (−100 mV/dec) for the two cluster compounds in a limited potential region suggest that a primary electron transfer is rate limiting. In the potential region more negative than 0.64 V vs. NHE, a deviation due to the kinetics of adsorption of O_2 or a reaction product is observed, which would here become the rate-determining step. The limitation of the favorable adsorption site has also to be considered as a possible reason for the slowdown of reaction kinetics at high current densities. Again, the situation is similar to that observed with platinum.

IV. Discussion and Outlook

On the basis of our photoelectron spectra supported by electronic band structure calculations it can be concluded that electrons involved in the reduction of oxygen at the $Mo_{4.2}Ru_{1.8}Se_8$ interface are reacting through transition metal d states originating from the mixed $(Mo,Ru)_6$ cluster. Since metallic Ru[26] and the oxides of Ru and Mo[27] or RuS_2[28] are catalytically little active for oxygen reduction in acidic medium, it is reasonable to assume, to a significant extent, that these cluster units are involved in the oxygen reduction catalysis and not dissociated into components. This is additionally confirmed by photoelectron spectroscopic data, which show that under conditions of oxygen reduction there is no evidence for oxide formation since there is no observable chemical shift of Mo and Ru.

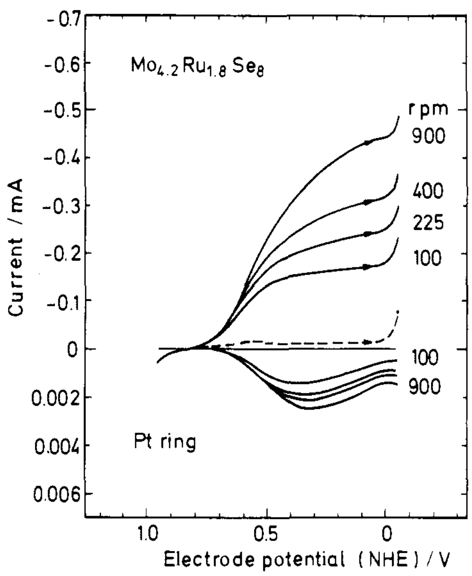

Figure 10. Current-potential curves for the reduction of O_2 at a rotating $Mo_{4.2}Ru_{1.8}Se_8$ disk-platinum ring electrode at different rotation rates. Electrolyte 0.5 M H_2SO_4 was saturated with O_2. Disk electrode potential was scanned at 5 mV s^{-1}. Ring electrode was potentiostated at +1.44 V. Dashed curve shows the background in nitrogen saturated solution. The collection factor is 0.31.

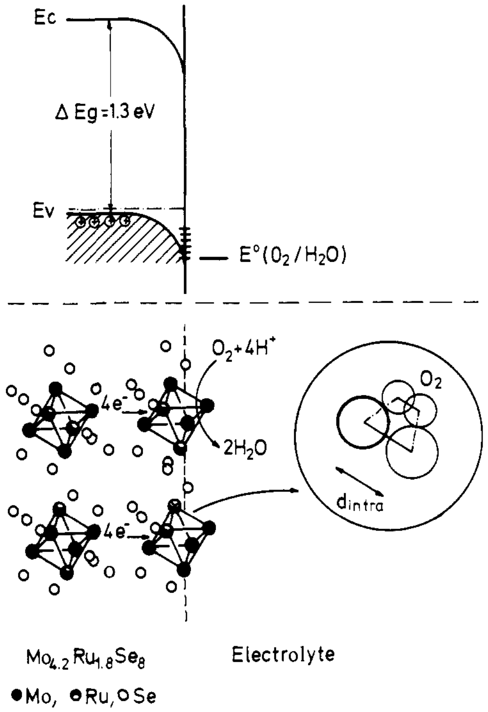

Figure 11. Schematic energy and molecular representation of the semiconducting $Mo_{4.2}Ru_{1.8}Se_8$ cluster and the redox couple (O_2/H_2O) at the interface under charge transfer condition. The insert shows a supposed interaction of molecular oxygen of the bridge type at two adjacent transition-metal atoms.

A cathodic photocurrent, and energy gap of E_g = 1.3 eV determined from the photoelectrochemical spectrum and a Mo:Ru ratio of 4.2:1.8, which yields an electron count of 23.6 per cluster unit (which is smaller than 24 needed for an ideally intrinsic semiconductor), characterizes the $Mo_{4.2}Ru_{1.8}Se_8$ compound as a degenerated p-type semiconductor with a hole concentration of the order of 5 × 10^{20} cm^{-3} (estimated from stoichiometry). The electronic scheme of this electrode during oxygen reduction is shown in Figure 11 together with a presentation of the arrangment of clusters toward the interface and a molecular representation

---

(25) (a) Bagotskii, V. S.; Lukyanycheva, V. I.; Leites, S. Sch. *Electrokhimiya* **1978**, *14*, 159. (b) Huang, J. C.; Sen, R. K.; Yeager, E. J. *Electrochem. Soc.* **1979**, *126*, 786.

(26) *Encyclopedia of electrochemistry of the elements*; Bard, A. J., Ed.; Marcel Dekker, Inc.; New York, 1976; Vol VI, p 291.

(27) Horkans, H.; Schafer, M. W. *J. Electrochem. Soc.* **1977**, *124*, 1196, 1202.

(28) Piazza, S.; Kühne, H.-M.; Tributsch, H. *J. Electroanal. Chem.* **1985**, *196*, 53.

of the probable oxygen–transition-metal cluster interaction. The following details have to be taken into account: Due to the high concentration of holes in the valence band the penetration depth of the space charge layer into the cluster material will be low. Assuming a hole concentration of 5×10^{20} cm^{-3}, $\epsilon = 10$, and $U = 1$ V, a space charge layer width of about $d = 15$ Å can be estimated. The oxygen reduction starts when the Fermi level of the electrode is 0.35 V above the thermodynamic redox potential of the O_2/H_2O redox couple. Under such conditions all weakly bonding d states in the valence band should be statistically occupied in an ideal electrode–electrolyte interface. We do, however, not know whether the electronic energies of cluster states in the surface are shifted toward higher energies due to a partial lack of Se ligands. In such a situation, surface cluster states could only partially be occupied with electrons during catalysis. However, we consider this case improbable since the metallic $Ni_xMo_6Te_8$ also contains clusters with an electrton count different from 24 e$^-$, but it is catalytically only a moderately active compound.

It is more likely that the oxygen reduction of a catalytically well performing $Mo_{4.2}Ru_{1.8}Se_8$ electrode starts with a cluster containing nearly 24 e$^-$ (i.e., in which all or most weakly bonding d states are filled with electrons). Under these conditions the intracluster bond distance d_1 (Figure 1) has a minimum value of $d_1 = 2.710$ Å (compared to $d_1 = 2.837$ Å as for Mo_6Se_8 after extraction of four electrons). It is reasonable to assume that molecular oxygen will start interacting with a particular transition metal atom of a cluster and during electron transfer assume a bridge type bonding to two adjacent transition metal atoms of the same cluster (molecular scheme in Figure 11) similar to bridge models discussed in the literature.[23] The reaction product of the primary step of electron transfer is therefore not O_2^- but reduced oxygen in chemical interaction with the transition metal cluster.

This complex between the reduced oxygen molecule and the cluster must be the key to the systems with favorable catalytic behavior. As a consequence of electron transfer from the transition-metal cluster to the chemisorbed oxygen molecule, two distinct phenomena are to be expected. One is that the transition-metal distance d_1 will increase thus possibly facilitating the breaking of the –O–O– bond liberating OH$^-$ ions. This mechanism is based on the correlation between the formal number of the valence electron in the cluster and the metal–metal bonding distances within the cluster, which is known from systematic studies reported elsewhere.[29] The second would be an expected upward shift of electronic levels due to a positive charging of the cluster. Due to the semiconducting properties of the material with a Fermi level above the edge of the valence band a complete refilling of the cluster with electrons (e.g., by tunneling) is to be expected even for cluster levels shifted a certain energetic distance upwards into the forbidden energy region. This may be one reason for the improvement of catalytic activity parallel with a change from metallic to increasingly semiconducting properties. The Fermi level within a metallic cluster compound (e.g., $Ni_xMo_6Te_8$) will maintain partially empty metal electron states for the surface transition metal cluster because the potential drop at the cluster compound/electrolyte interface will always occur in the Helmholtz layer at the surface of the material. The energy of the cluster states will therefore shift with the Fermi level without a significant change of electron occupation, when the electrode potential is varied. To be more specific, in a metal electrode, electrons will, during an electron exchange reaction, be transferred near the Fermi level, in a semiconductor electrode near the edge of an energy band. In addition, the reacting species in the interface can assume positions within the energy range of the forbidden energy region, where they can have lifetimes and reaction rates different from those when facing a continuum of empty or occupied electronic states of a metal. But these theoretical conclusions on the kinetic and energetic aspects of oxygen reduction at cluster compounds will need experimental confirmation. Other reaction possibilities, such as, for example, reported in ref 23, should also be taken into consideration.

Considering the difficulties which have been encountered for the last decades by many authors during the search for improved oxygen electrodes, semiconducting transition-metal cluster compounds appear to offer promising new research perspectives. Especially the role of transition-metal clusters as reservoirs for multielectron exchange at a stabilized electrochemical potential needs special consideration. Further research with transition-metal cluster materials of systematically varied stoichiometry will be needed to improve our understanding of the complicated process of oxygen reduction.

As judged from our present electrochemical work $Mo_{6-x}Ru_xSe_8$ could in principle compete with Pt as a catalyst in acid fuel cells at a considerable cost reduction. However, since only little is known about material and interfacial properties, scientific knowledge and technical experience on this compound needs first to be increased.

Acknowledgment. One of us (N.A.V.) gratefully acknowledges financial support from the Alexander von Humboldt Foundation. The authors thank Dr. R. Baillif (Geneva) for supplying the Ru-substituted samples and Dr. R. Könenkamp and Dr. W. Hofmann for assistance in the resistivity and electron microscopic measurements, respectively. The work was in part supported by a grant of the BMFT.

---

(29) Yvon, K. In *Superconductivity in Ternary Compounds I*; Fischer, Ø., Maple, M. B., Eds.; Springer Verlag: West Berlin, 1982; p 87.